PHYSICAL REVIEW E **80**, 030801(R) (2009)

Deformation mechanism of nanocomposite gels studied by contrast variation small-angle neutron scattering

Toshihiko Nishida,[1] Hitoshi Endo,[1] Noboru Osaka,[1] Huan-jun Li,[2] Kazutoshi Haraguchi,[2] and Mitsuhiro Shibayama[1]
[1]*Neutron Science Laboratory, Institute for Solid State Physics, The University of Tokyo, Tokai, Ibaraki 319-1106, Japan*
[2]*Kawamura Institute of Chemical Research, 631 Sakada, Sakura-shi, Chiba 285-0078, Japan*
(Received 10 June 2009; published 14 September 2009)

Contrast-variation small-angle neutron scattering (CV-SANS) was applied to investigate the deformation mechanism of high-performance nanocomposite polymer hydrogels (NC gels) consisting of polymer chains and inorganic clay platelets. Anisotropic SANS functions were obtained at various stretching ratios, λ's up to $\lambda=9$ and were decomposed to three partial structure factors, $S_{ij}(Q_\parallel,Q_\perp)$. Here, the subscripts i and j denote the polymer (P) or clay (C) and $Q_\parallel$ and $Q_\perp$ are the magnitude of the scattering vectors along and perpendicular to the stretching directions, respectively. $S_{CC}(Q_\parallel,Q_\perp)$ and $S_{PP}(Q_\parallel,Q_\perp)$ suggested that the orientation of clay platelets saturated by $\lambda\approx 3$, while the polymer chain stretching continued by further stretching. On the other hand, $S_{CP}(Q_\parallel,Q_\perp)$, only available by CV-SANS, indicated the presence of a polymer-enriched layer adsorbed to clay surface, which are responsible for large extensibility of NC gels over 1000% strain and large toughness exceeding 780 kPa.

DOI: 10.1103/PhysRevE.80.030801 PACS number(s): 81.05.Lg, 61.05.fg, 62.20.F−, 81.40.Lm

Polymer nanocomposites (PNs) are hybrid materials synthesized by incorporating nanoparticles into polymer matrix. A typical example is a tire, which has been used for more than 100 years [1]. Nanoparticles in PNs reinforce the mechanical properties as a filler. In spite of enormous efforts by experiments, theories, and simulations [2], the understanding of filler reinforcement has been still limited. One of the reason is a lack of the information at the polymer-filler interface under deformed state. Hence, it is important to carry out *in situ* investigations of PNs under deformation. Contrast-variation small-angle neutron scattering (CV-SANS) is one of powerful tools to explore the structure of multicomponent systems in nanoscopic order because it allows us to decompose the scattering intensities obtained at various scattering contrasts to partial structure factors. In the present Rapid Communication, we focus on structural change in polymer-nanoparticle interface by applying CV-SANS method to anisotropic soft matter systems.

Recently, nanocomposite hydrogels (NC gels), consisting of organic polymers, inorganic clay nanoparticles, and a large amount of water, were reported [3]. NC gels are prepared by radical polymerization of N-isopropylarylamide in the presence of laponite XLG $\{[Mg_{5.34}Li_{0.66}Si_8O_{20}(OH)_4]Na_{0.66}\}$. The clay is an assembly of platelets with ca. 150 Å in radius and 10 Å in thickness. NC gels have extraordinarily tough mechanical properties. Figure 1 shows stress-stretching ratio curves of a typical NC gel (NC15) and of a chemically crosslinked poly(N-isopropylacrylamide) (PNIPA) gel having a similar polymer concentration (OR3) together with a cartoon of NC gel. The clay and polymer concentrations were 0.15 mol/L (114.5 g/L) and 1 mol/L (113 g/L), respectively. The crosslinker (N,N,N′,N′-methylenbis acrylamide) concentration of OR3 was 3 mol % relative to NIPA monomer. $\lambda(l/l_0)$ is the stretching ratio, and l_0 and l are the sample lengths before and after stretching. As shown in the figure, NC15 exhibits high mechanical properties such as a rubber ring in spite of its low polymer concentration, i.e., approximately 10 wt % and absence of chemical crosslinkers. The maximum strain $(\lambda-1)$ and the stress at break of NC15 are over 1100% and 780 kPa, which are 50 and 80 times as large as those of PNIPA gel, respectively.

In our previous works, it was clarified that the clay platelets play as two dimensional crosslinkers [3–7]. However, information on the filler-polymer interface and the orientation of clay platelets and polymer chains, which are keys to understand the unique properties of NC gels, have not been obtained. In this Rapid Communication, we apply CV-SANS to investigate anisotropic scattering patterns, extract partial scattering functions, and carry out quantitative analyses of deformation mechanism of NC gels.

SANS experiments were performed at the two-dimensional (2D) SANS instrument (SANS-U), Neutron Science Laboratory, the University of Tokyo. The neutron wavelength was 7.0 Å and its distribution was approximately 10% [8]. The sample-to-detector distance (SDD) was 2 and 8 m. Prepared gels with various D_2O/H_2O fractions, the vol-

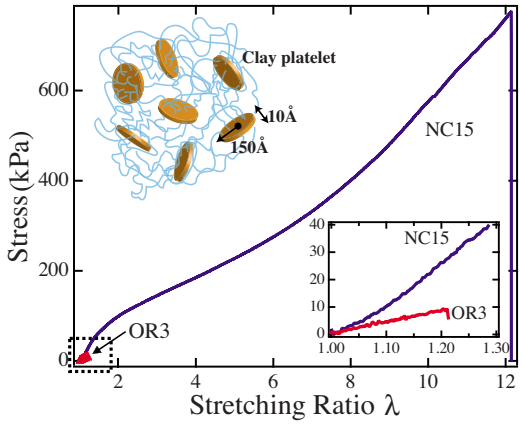

FIG. 1. (Color online) Stress stretching-ratio curves of NC gel (NC15) and chemically crosslinked PNIPA gel (OR3). Inset: stress-strain curve at a low stretching ratio region. A cartoon of NC gel is also shown.

 ©2009 The American Physical Society

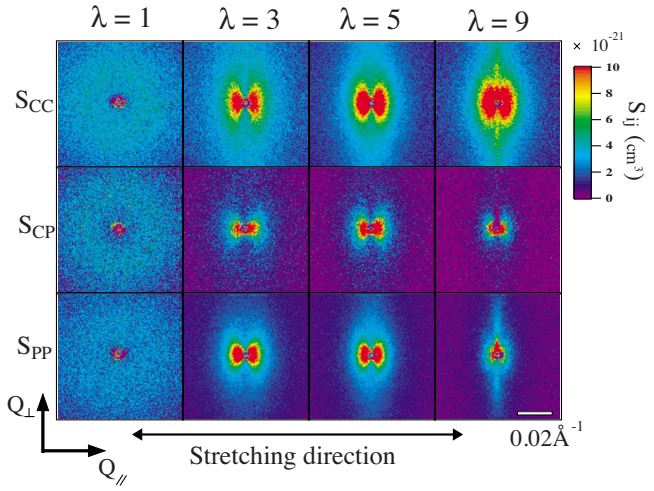

FIG. 2. (Color online) Two-dimensional SANS partial structure factors for NC15 obtained by CV-SANS method; clay scattering S_{CC}, clay polymer cross term S_{CP}, polymer scattering S_{PP}. SDD is 8 m and λ is the stretching ratio.

ume fractions of D_2O being f_{D2O}, were set to a custom-made stretching device. The stretching experiment was conducted with the same manner as was employed in the previous paper [6,7]. The sample was stretched stepwise up to $\lambda=9$ (i.e., $\lambda=1,3,5,7,9$). After each stretching process, structural relaxation for 10 min was allowed before starting next SANS measurement. The temperature of the samples was regulated to be 20 °C with a water-circulating bath controlled with a Neslab RTE-111 thermocontroller with the precision of ±0.1 °C. The water content of the gel was maintained by keeping the humidity of the sample chamber.

The scattering intensity of NC gel is written by

$$I(Q) = \Delta\rho_C^2 S_{CC}(Q) + \Delta\rho_P^2 S_{PP}(Q) + 2\Delta\rho_C \Delta\rho_P S_{CP}(Q). \quad (1)$$

Here, $\Delta\rho_i$ indicates the scattering length density difference between the solvent and the component i [$i=C$(clay),P(polymer)]. $S_{ij}(Q)$s are the partial scattering functions (PSFs). The scattering length densities of the three components were calculated on the basis of their chemical formulas and mass densities and were confirmed experimentally [5]. $S_{CC}(Q)$ and $S_{PP}(Q)$ are called the self-terms, representing the self-correlations of clay and polymer, respectively. $S_{CP}(Q)$ is the so-called cross term, representing the cross correlation between clay and polymer. $S_{CP}(Q)$ reflects the interaction between clay and polymer in NC gel. In order to extract these three PSFs, five NC gel samples with different D_2O fractions were prepared, and five $I(Q)$s were obtained for each stretching ratio. The volume fractions of D_2O were $f_{D2O}=0$, 0.216, 0.7, 0.8, and 1.0. $S_{ij}(Q)$s are obtained by decomposing $I(Q)$s with the method of singular value decomposition. Thus evaluated $S_{ij}(Q)$s were used to reconstruct $I(Q)$s so as to examine the validity and accuracy of the decomposition. The details of contrast variation method is described in the previous paper [4,5].

Figure 2 shows the decomposed 2D-PSFs $S_{CC}(Q_\parallel,Q_\perp)$, $S_{PP}(Q_\parallel,Q_\perp)$, and $S_{CP}(Q_\parallel,Q_\perp)$ of uniaxially stretched NC gels (Q range; $0.005 \le Q \le 0.035$ Å^{-1}, SDD=8 m) at four stretching ratios ($\lambda=1,3,5,9$). Note that $S_{CC}(Q_\parallel,Q_\perp)$ and $S_{PP}(Q_\parallel,Q_\perp)$ can be easily obtained by SANS measurements with a condition of contrast matching, i.e., $\Delta\rho_P=0$ (polymer matched) or $\Delta\rho_C=0$ (clay matched). However, $S_{CP}(Q_\parallel,Q_\perp)$ can be obtained only by decomposition of $I(Q_\parallel,Q_\perp)$s. As clearly seen in the figure, the scattering pattern changes by stretching.

At $\lambda=1$, the scattering intensities are weak and the patterns are isotropic, suggesting that both clay platelets and polymer chains are oriented randomly in the NC gel. By stretching to $\lambda=3$, anisotropy appears in all PSFs, characterized by a butterfly pattern and an outer elliptic lobe pattern elongated in the perpendicular direction. The origin of the butterfly pattern in NC gel is completely different from those reported in the literature [9–11]. The elliptic pattern in $S_{CC}(Q_\parallel,Q_\perp)$ does not seem to change noticeably by further stretching. This behavior in $S_{CC}(Q_\parallel,Q_\perp)$ may indicate that clay orientation is saturated by $\lambda=3$. This is due to interblocking of clay platelets themselves because the interclay platelet distance (estimated to be 283 Å by stoichiometry) is shorter than the diameter of the platelets (≈300 Å). This SANS result is consistent with optical birefringence measurements on NC gels by Murata *et al.* [12]. The appearance of the central butterfly pattern is ascribed to the correlation between clay platelets. This pattern means that the average interclay platelet distances are different in the parallel and perpendicular directions. Macroscopically NC gel is stretched in the parallel direction and is compressed in the perpendicular direction.

$S_{PP}(Q_\parallel,Q_\perp)$, on the other hand, becomes more anisotropic by increasing λ. At $\lambda=9$, a strong streak pattern appears in the perpendicular direction, indicating that polymer chains are highly stretched in the parallel direction. It is quite important to note that $S_{CP}(Q_\parallel,Q_\perp)$ is positive and looks similar to $S_{CC}(Q_\parallel,Q_\perp)$ at $\lambda=3$. This indicates that there exists strong correlation between clay and polymer and the clay-polymer cross term behaves similar to the clay-clay self term. A most plausible scenario explaining this phenomenon is that there exists a polymer-enriched layer on the surface of clay platelets and the layer itself orients simultaneously with the clay platelets. However, such synchronized orientation is lost by further increasing $\lambda>3$ as seen by fading out of the pattern in $S_{CP}(Q_\parallel,Q_\perp)$ at $\lambda=9$. Hence, it is deduced that the polymer-enriched layer is peeled off by stretching.

In order to evaluate the 2D-PSFs in Fig. 2 more quantitatively and confirm the above mentioned scenario, we carried out a series of curve fitting with theoretical scattering functions for sector-averaged PSFs. Figure 3 shows the laboratory coordinate showing the relationship between the sample and the scattering vector. The incident neutron beam propagates along the x axis and the stretching direction is taken along the z axis. The clay platelet, with its principal axis in the z_1 direction, is oriented randomly or preferentially with respect to the z axis by an angle α. Here, we assume that the clay platelet has a uniaxial symmetry with respect to the z axis. Hence, the orientation with respect to the azimuthal angle Ω can be preaveraged. The detector plane is placed in the O-zy plane. The sector average of $S_{ij}(Q_\parallel,Q_\perp)$ was taken with the angle μ with the sector of $-20° \le \mu \le 20°$ and $70° \le \mu \le 110°$ in the parallel and perpendicular to stretch-

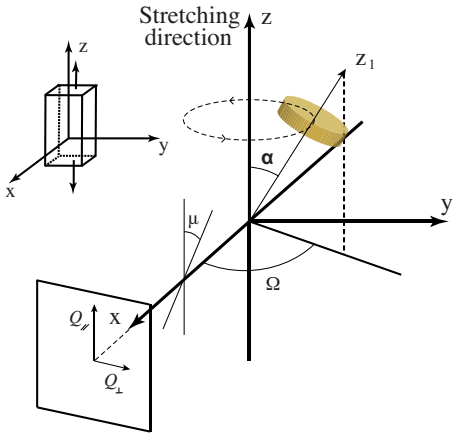

FIG. 3. (Color online) Laboratory coordinate showing the relationship among the clay orientation, the stretching direction, and the detector plane.

ing directions, respectively. The theoretical scattering function is given by

$$P_c(Q) = \int_{\pi/2-\alpha_0}^{\pi/2+\alpha_0} \{A_c(Q;\alpha)\}^2 \sin\alpha d\alpha, \tag{2}$$

where α_0 is the cut-off angle of the orientation (=90° for random orientation and ≪90° for a preferred orientation) and A_c is the scattering amplitude of a clay platelet given by

$$A_c(Q;\alpha) = V_c \frac{2J_1(QR_c \sin\alpha)}{QR_c \sin\alpha} \frac{\sin\{Q(d_c/2)\cos\alpha\}}{\{Q(d_c/2)\cos\alpha\}}. \tag{3}$$

Here, $J_1(x)$ is the cylindrical Bessel function of first order and V_c is the volume of a platelet, i.e., $V_c = \pi R_c^2 d_c$. The interplatelet interference function for platelets, $\tilde{S}_c(Q)$, was assumed to be given by a Percus-Yevick (PY) interference function for hard sphere model [13–15], $\tilde{S}_{PY}(Q, R_{PY}, \phi_{PY})$ with an equivalent hard-core radius, R_{PY} and its volume fraction, ϕ_{PY}, i.e.,

$$\tilde{S}_c(Q) \approx 1 + \frac{\langle A_c(Q;\alpha)\rangle^2}{P_c(Q)} \{\tilde{S}_{PY}(Q, R_{PY}, \phi_{PY}) - 1\}, \tag{4}$$

with $\langle A_c(Q;\alpha)\rangle = \int_{\pi/2-\alpha_0}^{\pi/2+\alpha_0} A_c(Q;\alpha)\sin\alpha d\alpha$. Hence, the partial scattering function of clay, $S_{CC}(Q)$, is given by $S_{CC}(Q) = n_c \tilde{S}_c P_c(Q)$, where n_c is the number density of the clay platelets. Similarly to S_{CC}, S_{PP} is defined as a sum of two-scattering functions originating from the polymer-enriched layers $S_p(Q)$ and the matrix $S_{\text{matrix}}(Q)$. The former is a scattering function for a shell with the shell thickness of ζ, and the latter is simply assumed to be an Ornstein-Zernike function with the correlation length, ξ. The cross-term S_{CP} is given by a product of the scattering amplitude functions of clay and polymer. The thickness of the absorbed layer ζ and the correlation length of the polymer matrix ξ for under deformed state were evaluated to be $\zeta = 11.7$ Å and $\xi = 171$ Å [5]. The details of the scattering model and analyses are discussed by Endo *et al.* [5].

The sector-averaged scattering functions $S_{CC,\parallel}(Q_\parallel)$ and $S_{CC,\perp}(Q_\perp)$ are plotted in Fig. 4. $S_{CC,\parallel}(Q_\parallel)$ shows a jumpwise

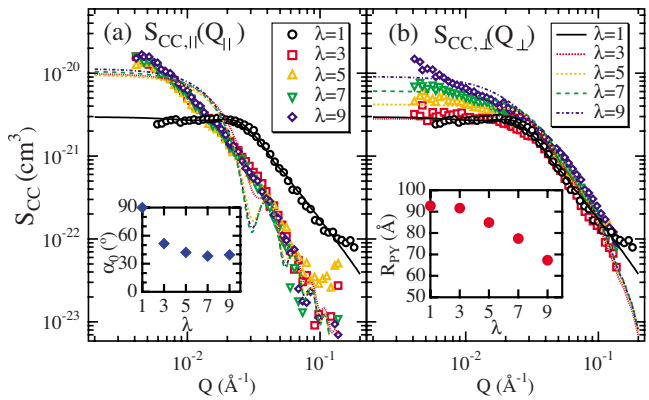

FIG. 4. (Color online) The sector-averaged scattering functions (a) $S_{CC,\parallel}(Q_\parallel)$ and (b) $S_{CC,\perp}(Q_\perp)$ in the z and y directions, respectively. Solid curves are fitting results obtained by the PY model function for oriented disks. Left inset: the stretching ratio dependence of orientation freedom α. Right inset: the stretching ratio dependence of the PY radius.

change by increasing $\lambda = 1-3$ and then becomes independent of λ, indicating that clay orientation is saturated by $\lambda = 3$. The $S_{CC,\parallel}$ and $S_{CC,\perp}$ are χ^2 fitted by using Eqs. (2)–(4). The fitting curve for $S_{CC,\parallel}$ with $\lambda \geq 3$ does not reproduce very well at low-Q region, which indicates that the PY structure factor is too simple to express the clay-clay interaction in a parallel direction. The inset of Fig. 4(a) shows the cut-off angle of clay orientation α_0, which decreases from 90° (random orientation) to 50° (a preferred orientation). In the perpendicular direction, $S_{CC,\perp}(Q_\perp)$ in low Q region (≤0.02 Å) increases with elongation. This means that the interplatelet interference function, $\tilde{S}_c$, increases in the low Q region with increasing λ in the perpendicular direction. This corresponds to a lowering in R_{PY} with λ as shown in the inset of Fig. 4(b) and suggests that clay platelets becomes closer to each other with a preferred orientation and compression occurs in the perpendicular direction by increasing λ.

Figure 5 shows the averaged scattering functions for the cross terms, $S_{CP,\parallel}(Q_\parallel)$ and $S_{CP,\perp}(Q_\perp)$. First of all, it is noteworthy that these cross terms are positive in the whole Q range studied in this work. This means that there exist attrac-

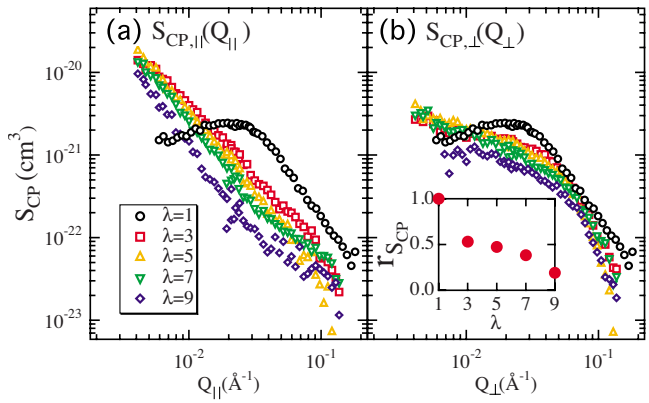

FIG. 5. (Color online) The sector-averaged scattering functions $S_{CP,\parallel}(Q_\parallel)$ and $S_{CP,\perp}(Q_\perp)$ in z and y direction, respectively. Inset in (b): λ dependence of the ratio $r_{S_{CP}} \equiv S_{CP}(Q)/S_{CP}(Q)_{\lambda=1}$.

tive interactions between clay platelets and polymer chains. For NC15 with $\lambda=1$, the thickness ζ and the local polymer fraction in the layer ϕ_{pl} were evaluated by curve fitting of $S_{ij}(Q)$ to be 11.6 Å and 0.40, respectively. Since the polymer volume fraction in the polymer matrix ϕ_{pex} is 0.071, the polymer concentration in the adsorbed layer is more than five times higher than that in the matrix.

For $\lambda \geq 3$, the magnitude of S_{CP}s decreases by stretching. It is interesting to note that both $S_{CP,\parallel}(Q_{\parallel})$s and $S_{CP,\perp}(Q_{\perp})$s decrease with $\lambda(\geq 3)$, respectively, by keeping more or less the same shape of the scattering function. Hence, it is deduced that the lowering of magnitude simply means a decrease in the polymer concentration in the polymer enriched layer, in other word, a decrease in the polymer concentration in the "polymer-enriched layer," ϕ_{pl}. The quantitative data analysis with concrete model fitting for S_{CP} is currently under consideration. Instead, the ratio $r_{S_{CP}} \equiv \overline{S_{CP}(Q)}_{\lambda} / \overline{S_{CP}(Q)}_{\lambda=1}$ was evaluated in order to estimate the change in the adsorbed layer. Here, $\overline{\cdots}$ means the integrated intensity of $S_{CP}(Q)$ in the 2D PSF S_{CP}s of Fig. 2 in the Q range of $0.027 \leq (Q_{\parallel}, Q_{\perp}) \leq 0.067$ Å^{-1}. Since the summation of the scattering intensity is proportional to the volume of polymer enriched layer, $r_{S_{CP}}$ represents the change in polymer concentration in the enriched layer. As shown in the figure, the polymer concentration in the enriched layer indeed deceases from unity to approximately 19% by $\lambda=1-9$. Therefore, it is again concluded that a significant fraction of polymer chains in the layer is peeled off from the clay surface by stretching.

In conclusion, we have succeeded in applying CV-SANS to anisotropic SANS patterns for elucidation of the deformation mechanism of NC gels (NC15) under uniaxial stretching. It is concluded that clay platelets orient parallel to the stretching direction and the orientation is saturated by $\lambda=3$ with the allowance angle of $\pm 40°$. Further structural change occurs preferentially in the polymer phase, i.e., stretching of polymer chains along the stretching direction as well as peeling off of polymer chains from the adsorbed layer. This peeling-off phenomenon is characteristic and is one of the main reasons of the high extensibility and high modulus of NC gels.

This work was partially supported by the Ministry of Education, Science, Sports and Culture, Japan [Grant-in-Aid for Scientific Research, Grants No. 18205025 and No. 18068004, Grant-in-Aid for Scientific Research (A), 2006-2008, No. 18205025, and for Scientific Research on Priority Areas, 2006-2010, No. 18068004]. The SANS experiment was performed with the approval of Institute for Solid State Physics, The University of Tokyo (Proposals No. 7628 and No. 8622) at Japan Atomic Energy Agency, Tokai, Japan.

[1] E. Guth, J. Appl. Phys. **16**, 20 (1945).
[2] J. E. Mark, J. Phys. Chem. B **107**, 903 (2003).
[3] K. Haraguchi and T. Takehisa, Adv. Mater. **14**, 1120 (2002).
[4] S. Miyazaki, H. Endo, T. Karino, and M. Shibayama, Macromolecules **40**, 4287 (2007).
[5] H. Endo, S. Miyazaki, and M. Shibayama, Macromolecules **41**, 5406 (2008).
[6] M. Shibayama, T. Karino, S. Miyazaki, S. Okabe, T. Takehisa, and K. Haraguchi, Macromolecules **38**, 10772 (2005).
[7] S. Miyazaki, T. Karino, H. Endo, K. Haraguchi, and M. Shibayama, Macromolecules **39**, 8112 (2006).
[8] S. Okabe, T. Karino, M. Nagao, S. Watanabe, and M. Shibayama, Nucl. Instrum. Methods Phys. Res. A **572**, 853 (2007).
[9] A. Onuki, J. Phys. II **2**, 45 (1992).
[10] S. Panyukov and Y. Rabin, Phys. Rep. **269**, 1 (1996).
[11] C. Rouf, J. Bastide, J. M. Pujol, F. Schosseler, and J. P. Munch, Phys. Rev. Lett. **73**, 830 (1994).
[12] K. Murata and K. Haraguchi, J. Mater. Chem. **17**, 3385 (2007).
[13] M. Shibayama, S. Nomura, T. Hashimoto, and E. L. Thomas, J. Appl. Phys. **66**, 4188 (1989).
[14] J. K. Percus and G. J. Yevick, Phys. Rev. **110**, 1 (1958).
[15] M. Kotlarchyk and S.-H. Chen, J. Chem. Phys. **79**, 2461 (1983).